

Feature Affinity Assisted Knowledge Distillation and Quantization of Deep Neural Networks on Label-Free Data

Zhijian Li, Biao Yang, Penghang Yin, Yingyong Qi, and Jack Xin

Abstract—In this paper, we propose a feature affinity (FA) assisted knowledge distillation (KD) method to improve quantization-aware training of deep neural networks (DNN). The FA loss on intermediate feature maps of DNNs plays the role of teaching middle steps of a solution to a student instead of only giving final answers in the conventional KD where the loss acts on the network logits at the output level. Combining logit loss and FA loss, we found that the quantized student network receives stronger supervision than from the labeled ground-truth data. The resulting FAQD is capable of compressing model on label-free data, which brings immediate practical benefits as pre-trained teacher models are readily available and unlabeled data are abundant. In contrast, data labeling is often laborious and expensive. Finally, we propose a fast feature affinity (FFA) loss that accurately approximates FA loss with a lower order of computational complexity, which helps speed up training for high resolution image input.

Index Terms—Quantization, Convolutional Neural Network, Knowledge Distillation, Model Compression, Image Classification

I. INTRODUCTION

Quantization is one of the most popular methods for deep neural network compression, by projecting network weights and activation functions to lower precision thereby accelerate computation and reduce memory consumption. However, there is inevitable loss of accuracy in the low bit regime. One way to mitigate such an issue is through knowledge distillation (KD [10]). In this paper, we study a feature affinity assisted KD so that the student and teacher networks not only try to match their logits at the output level but also match feature maps in the intermediate stages. This is similar to teaching a student through intermediate steps of a solution instead of just showing the final answer (as in conventional KD [10]). Our method does not rely on ground truth labels while enhancing student network learning and closing the gaps between full and low precision models.

A. Weight Quantization of Neural Network

Quantization-aware training (QAT) searches the optimal model weight in training. Given an objective L , the classical

Zhijian Li, Biao Yang, Yingyong Qi, and Jack Xin are with Department of Mathematics, University of California, Irvine, CA, USA

Penghang Yin is with Department of Mathematics and Statistics, State University of New York at Albany, Albany, NY, USA

Corresponding author: Zhijian Li (e-mail: zhijil2@uci.edu)

This work was partly supported by NSF grants DMS-1924935, DMS-1952644, DMS-2151235, DMS-2208126; and a Qualcomm faculty award.

QAT scheme ([6], [21]) is formulated as

$$\begin{cases} w^{t+1} = w^t - \nabla_u L(u^t), \\ u^{t+1} = \text{Quant}(w^{t+1}), \end{cases} \quad (1)$$

where Quant is projection to a low precision quantized space. Yin et al. [28] proposed BinaryRelax, a relaxation form of QAT, which replaces the second update of (1) by

$$u^{t+1} = \frac{w^{t+1} + \lambda^{t+1} \text{Quant}(w^{t+1})}{1 + \lambda^{t+1}}, \quad (2)$$

$$\lambda^{t+1} = \eta \lambda^t \quad \text{with } \eta > 1.$$

Darkhorn et al. [7] further improved (2) by designing a more sophisticated learnable growing scheme for λ^t and factoring a learnable parameter into Proj(\cdot). Polino et al. [19] proposed quantized distillation (QD), a QAT framework that leverages knowledge distillation for quantization. Under QD, the quantized model receives supervision from both ground truth (GT) labels and a trained teacher in float precision (FP). The objective function has the generalized form ($\alpha \in (0, 1)$):

$$\mathcal{L}_{QD} = \alpha \mathcal{L}_{KD} + (1 - \alpha) \mathcal{L}_{GT} \quad (3)$$

where \mathcal{L}_{KD} is Kullback–Leibler divergence (KL) loss, and \mathcal{L}_{GT} is negative log likelihood (NLL) loss. In order to compare different methods fairly, we introduce two technical terms: end-to-end quantization and fine-tuning quantization. End-to-end quantization is to train a quantized model from scratch, and fine-tuning quantization is to train a quantized model from a pre-trained float precision (FP) model. With the same method, the latter usually lands a better result than the former. Li et al. [15] proposed a mixed quantization (a.k.a. BRECCQ) that takes a pre-trained model and partially retrains the model on a small subset of data. We list the performance of some previous works of weight quantization, which will serve as baselines for this work.

Method	1-bit	2-bit	4-bit
Model: ResNet20			
QAT ([6], [21])	87.07%	90.26%	91.47%
BinaryRelax [28]	88.64%	90.47%	91.75%
QD [19]	89.06%	90.86%	91.89%
DSQ [8]	90.24%	91.06%	91.92%
BRECCQ [15]	N/A	81.31%	83.98%

TABLE I: Quantization accuracies of some existing quantization-aware training methods on CIFAR-10 dataset. All methods except BRECCQ are end-to-end.

B. Activation Quantization

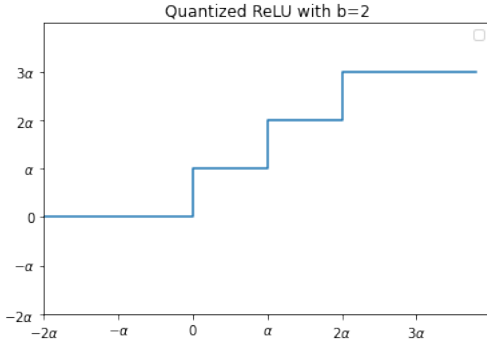


Fig. 1: Plot of 2-bit quantized ReLU $\sigma(x, \alpha)$

In addition to weight quantization, the inference of neural networks can be further accelerated through activation quantization. Given a resolution $\alpha > 0$, a quantized ReLU activation function of bit-width $b \in \mathbb{N}$ is formulated as:

$$\sigma(x, \alpha) = \begin{cases} 0 & x < 0 \\ k\alpha & (k-1)\alpha \leq x < k\alpha, \quad 1 \leq k \leq 2^b - 1 \\ (2^b - 1)\alpha & x \geq (2^b - 1)\alpha \end{cases} \quad (4)$$

where the resolution parameter α is learned from data. A plot of 2-bit quantized ReLU is shown in figure 1. However, such quantized activation function leads to vanished gradient during training, which makes the standard backpropagation inapplicable. Indeed, it is clear that $\frac{\partial \sigma}{\partial x} = 0$ almost everywhere. Bengio et al. [2] proposed to use a straight through estimator (STE) in backward pass to handle the zero gradient issue. The idea is to simply replace the vanished $\frac{\partial \sigma}{\partial x}$ with a non-trivial derivative $\frac{\partial \tilde{\sigma}}{\partial x}$ of a surrogate function $\tilde{\sigma}(x, \alpha)$. Theoretical studies on STE and convergence vs. recurrence issues of training algorithms have been conducted in ([17], [27]). Among a variety of STE choices, a widely-used STE is the x -derivative of the so-called clipped ReLU [3] $\tilde{\alpha}(x, \alpha) = \min\{\max\{x, 0\}, (2^b - 1)\alpha\}$, namely,

$$\frac{\partial \tilde{\sigma}}{\partial x} = \begin{cases} 1 & 0 < x < (2^b - 1)\alpha \\ 0 & \text{else.} \end{cases}$$

In addition, a few proxies of $\frac{\partial \sigma}{\partial \alpha}$ have been proposed ([4], [29]). In this work, we follow [29] and use the three-valued proxy:

$$\frac{\partial \sigma}{\partial \alpha} \approx \begin{cases} 0 & x \leq 0 \\ 2^{b-1} & 0 < x < (2^b - 1)\alpha \\ 2^b - 1 & x \geq (2^b - 1)\alpha. \end{cases} \quad (5)$$

C. Knowledge Distillation

Several works have proposed to impose closeness of the probabilistic distributions between the teacher and student networks, e.g. similarity between feature maps. A flow of solution procedure (FSP) matrix in [26] measures the information exchange between two layers of a given model. Then l_2 loss regularizes the distance between FSP matrices of teacher and student in knowledge distillation. An attention transform

(AT) loss [30] directly measures the distance of feature maps outputted by teacher and student, which enhances the learning of student from teacher. Similarly, feature affinity (FA) loss [24] measures the distance of two feature maps. In a dual learning framework for semantic segmentation [24], the FA loss is applied on the output feature maps of a segmentation decoder and a high-resolution decoder. In [25], FA loss on multi-resolution paths also improves light weight semantic segmentation. Given two feature maps with the same height and width (interpolate if different), $\mathbf{F}^S \in \mathbb{R}^{C_1 \times H \times W}$ and $\mathbf{F}^T \in \mathbb{R}^{C_2 \times H \times W}$, we first normalize the feature map along the channel dimension. Given a pixel of feature map $F_i \in \mathbb{R}^C$, we construct an affinity matrix $\mathbf{S} \in \mathbb{R}^{WH \times WH}$ as:

$$\mathbf{S}_{ij} = \|\mathbf{F}_i - \mathbf{F}_j\|_\theta := \cos \theta_{ij} = \frac{\langle \mathbf{F}_i, \mathbf{F}_j \rangle}{\|\mathbf{F}_i\| \|\mathbf{F}_j\|},$$

where Θ_{ij} measures the angle between F_i and F_j . Hence, the FA loss measures the similarity of pairwise angular distance between pixels of two feature maps, which can be formulated as

$$L_{fa}(\mathbf{F}^S, \mathbf{F}^T) = \frac{1}{W^2 H^2} \|\mathbf{S}^T - \mathbf{S}^S\|_2^2. \quad (6)$$

D. Contributions

In this paper, our main contributions are:

- 1) We find that using mean squares error (MSE) gives better performance than KL on QAT, which is a significant improvement to QD ([19]).
- 2) We consistently improve the accuracies of various quantized student networks by imposing the FA loss on feature maps of each convolutional block. We also unveil the theoretical underpinning of feature affinity loss in terms of the celebrated Johnson-Lindenstrass lemma for low-dimensional embeddings.
- 3) We achieve state-of-art quantization accuracy on CIFAR-10 and CIFAR-100. Our FAQD framework *can train a quantized student network on unlabeled data*.
- 4) We propose a randomized Fast FA (FFA) loss to accelerate the computation of training loss, and prove its convergence and error bound.

II. FEATURE AFFINITY ASSISTED DISTILLATION AND QUANTIZATION

A. Feature Affinity Loss

In quantization setting, it is unreasonable to require that F^S is close to F^T , as they are typically in different spaces ($F^S \in \mathcal{Q}$ in full quantization) and of different dimensions. However, F^S can be viewed as a compression of F^T in dimension, and preserving information under such compression has been studied in compressed sensing. Researchers ([20], [22]) have proposed to compress graph embedding to lower dimension so that graph convolution can be computed efficiently. In K-means clustering problem, several methods ([1], [18]) have been designed to project the data into a low-dimensional space such that

$$\|\text{Proj}(\mathbf{x}) - \text{Proj}(\mathbf{y})\| \approx \|\mathbf{x} - \mathbf{y}\|, \quad \forall (\mathbf{x}, \mathbf{y}), \quad (7)$$

and so pairwise distances from data points to the centroids can be computed at a lower cost.

In view of the feature maps of student model as a compression of teacher’s feature maps, we impose a similar property in terms of pairwise angular distance:

$$\|\mathbf{F}_i^S - \mathbf{F}_j^S\|_\theta \approx \|\mathbf{F}_i^T - \mathbf{F}_j^T\|_\theta, \forall (i, j)$$

which is realized by minimizing the feature affinity loss. On the other hand, a Johnson–Lindenstrauss (JL [11]) like lemma can guarantee that we have student’s feature affinity matrix close to the teacher’s, provided that the number of channels of student network is not too small. In contrast, the classical JL lemma states that a set of points in a high-dimensional space can be embedded into a space of much lower dimension in such a way that the *Euclidean* distances between the points are nearly preserved. To tailor it to our application, we prove the following JL-like lemma in the angular distance case:

Theorem 2.1 (Johnson–Lindenstrauss lemma, Angular Case): Given any $\epsilon \in (0, 1)$, an embedding matrix $\mathbf{F} \in \mathbb{R}^{n \times d}$, for $k \in (16\epsilon^{-2} \ln n, d)$, there exists a linear map $T(\mathbf{F}) \in \mathbb{R}^{n \times k}$ so that

$$\begin{aligned} (1 - \epsilon)\|\mathbf{F}_i - \mathbf{F}_j\|_\theta &\leq \|T(\mathbf{F})_i - T(\mathbf{F})_j\|_\theta \\ &\leq (1 + \epsilon)\|\mathbf{F}_i - \mathbf{F}_j\|_\theta, \quad \forall 1 \leq i, j \leq n \end{aligned} \quad (8)$$

where $\|\mathbf{F}_i - \mathbf{F}_j\|_\theta = \frac{\langle \mathbf{F}_i, \mathbf{F}_j \rangle}{\|\mathbf{F}_i\| \|\mathbf{F}_j\|}$ is the angular distance.

It is thus possible to reduce the embedding dimension down from d to k , while roughly preserving the pairwise angular distances between the points. In a convolutional neural network, we can view intermediate feature maps as $\mathbf{F}^S \in \mathbb{R}^{HW \times C_1}$ and $\mathbf{F}^T \in \mathbb{R}^{HW \times C_2}$, and feature affinity loss will help the student learn a compressed feature embedding. The FA loss can be flexibly placed between teacher and student in different positions (encoder/decoder, residual block, etc.) for different models. In standard implementation of ResNet, residual blocks with the same number of output channels are grouped into a sequential layer. We apply FA loss to the features of such layers.

$$\mathcal{L}_{FA} = \sum_{l=1}^L L_{fa}(\mathbf{F}_l^T, \mathbf{F}_l^S)$$

where \mathbf{F}_l^T and \mathbf{F}_l^S are the feature maps of teacher and student respectively. For example, the residual network family of ResNet20, ResNet56, ResNet10, and ResNet164 have $L = 3$, whereas the family of ResNet18, ResNet34, and ResNet50 have $L = 4$.

B. Choice of Loss Functions

In this work, we propose two sets of loss function choices for the end-to-end quantization and pretrained quantization, where end-to-end quantization refers to having an untrained student model with randomly initialized weights. We investigate both scenarios of quantization and propose two different strategies for each.

The Kullback–Leibler divergence (KL) is a metric of the similarity between two probabilistic distributions. Given a

ground-truth distribution P , it computes the relative entropy of a given distribution Q from P :

$$\mathcal{L}_{KL}(P||Q) = \sum_{x \in \mathcal{X}} P(x) \ln \frac{P(x)}{Q(x)}. \quad (9)$$

While KD is usually coupled with KL loss ([10], [19]), it is not unconventional to choose other loss functions. Kim et al. [14] showed that MSE, in certain cases, can outperform KL in the classic teacher-student knowledge distillation setting. KL loss is also widely used for trade-off between accuracy and robustness under adversarial attacks, which can be considered as self-knowledge distillation. Given a classifier f , an original data point \mathbf{x} and its adversarial example \mathbf{x}' , TRADES [31] is formulated as

$$L_{TRADES} = \mathcal{L}_{CE}(f(\mathbf{x}), y) + \mathcal{L}_{KL}(f(\mathbf{x})||f(\mathbf{x}'))$$

Li et al. [16] showed that $L_{CE}(f(\mathbf{x}'), y)$ outperforms $\mathcal{L}_{KL}(f(\mathbf{x})||f(\mathbf{x}'))$ both experimentally and theoretically.

Inspired by the studies above, we conduct experiments on different choices of the loss function. We compare KD on quantization from scratch (end-to-end). As shown in table II, MSE outperforms KL in quantization.

Student	Teacher	1-bit	2-bit	4-bit
$\mathcal{L}_{KD} = \text{KL loss in (3)}$				
ResNet20	ResNet10	89.06%	90.86%	91.89%
$\mathcal{L}_{KD} = \text{MSE in (3)}$				
ResNet20	ResNet10	90.00%	91.01%	92.05%

TABLE II: Comparison of KL loss and MSE loss on CIFAR-10 data set. All teachers are pre-trained FP models, and all students are initial models (end-to-end quantization).

On the other hand, we find that KL loss works better for fine-tuning quantization. One possible explanation is that when training from scratch, the term $\ln \frac{P(x)}{Q(x)}$ is large. However, the derivative of logarithm is small at large values, which makes it converge slower and potentially worse. On the other hand, when $\frac{P(x)}{Q(x)}$ is close to 1, the logarithm has sharp slope and converges fast.

C. Feature Affinity Assisted Distillation and Quantization

Inspired by previous studies ([13], [15], [19]), we propose a feature affinity assisted quantized distillation (FAQD). The end-to-end quantization objective function is formulated as:

$$\begin{aligned} \mathcal{L} &= \alpha \mathcal{L}_{KD} + \beta \mathcal{L}_{FA} + \gamma \mathcal{L}_{GT} \\ &= \alpha \mathcal{L}_{MSE}(f^T(\mathbf{x}), f^S(\mathbf{x})) + \beta \sum_{l=1}^L L_{fa}(\mathbf{F}_l^T, \mathbf{F}_l^S) \\ &\quad + \gamma \mathcal{L}_{NLL}(f^S(\mathbf{x}), y). \end{aligned} \quad (10)$$

In fine-tuning quantization, we replace MSE loss in (10) by KL divergence loss. In FAQD, the student model learns not only the final logits of the teacher but also the intermediate extracted feature maps of the teacher using feature affinity norm computed as in [24].

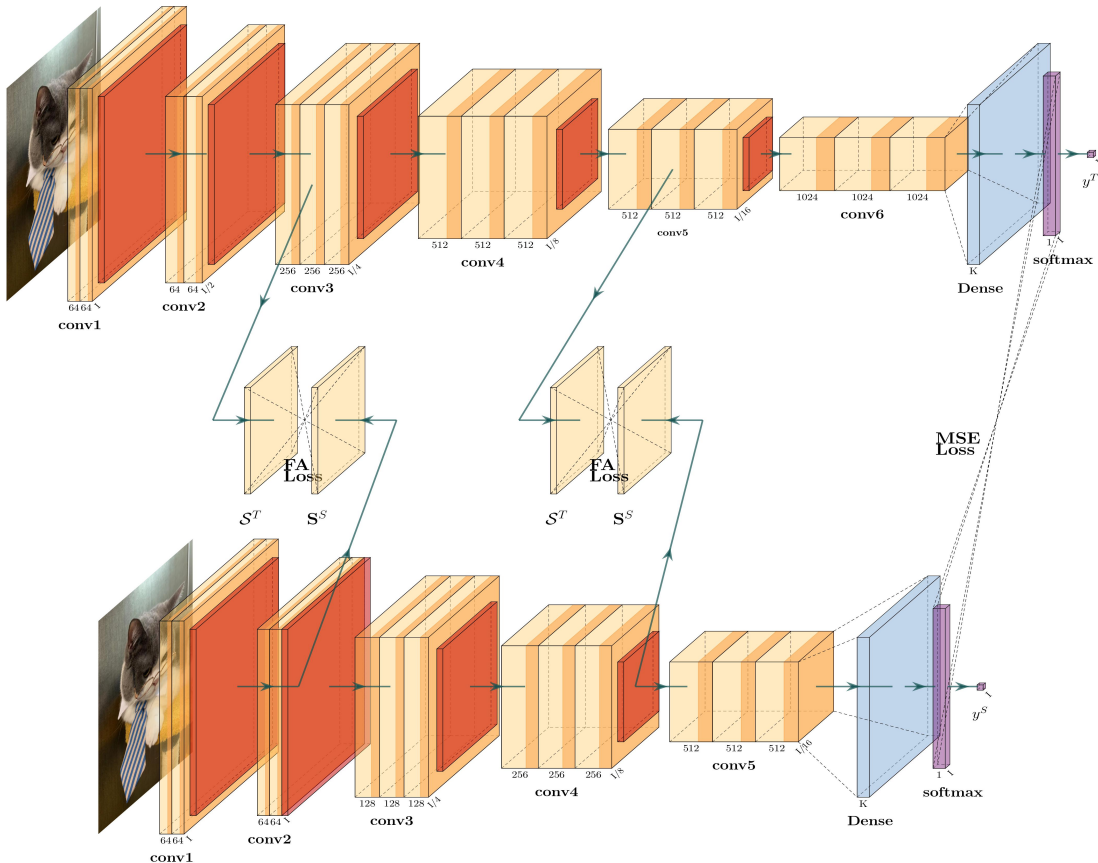


Fig. 2: FAQD framework. The intermediate feature maps are supervised by FA loss, and the raw logits by MSE loss.

In addition to (10), we also propose a label-free objective which does not require the knowledge of labels:

$$\mathcal{L}_{\text{label-free}} = \alpha \mathcal{L}_{MSE}(f^T(\mathbf{x}), f^S(\mathbf{x})) + \beta \sum_{l=1}^L \mathcal{L}_{fa}(\mathbf{F}_l^T, \mathbf{F}_l^S). \quad (11)$$

Despite the pre-trained computer vision models being available from cloud service such as AWS and image/video data abundantly collected, the data labeling is still expensive and time consuming. Therefore, a label-free quantization framework has significant value in the real world. In this work, we verify that the FA loss can significantly improve KD performance. The label-free loss in Eq. (11) can outperform the baseline methods in table I as well as the prior supervised QD in (3).

III. EXPERIMENTAL RESULTS

A. Weight Quantization

In this section we test FAQD on the dataset CIFAR-10. First, we experiment on fine-tuning quantization. The float precision (FP) ResNet110 teaches ResNet20 and ResNet56. The teacher has 93.91% accuracy, and the two pre-trained models have accuracy 92.11% and 93.31% respectively. While both SGD and Adam optimization work well on the problem, we found KL loss with Adam slightly outperform SGD in this scenario. The objective is

$$\mathcal{L} = \mathcal{L}_{KL} + \mathcal{L}_{FA}$$

for the label-free quantization. When calibrating the ground-truth label, the cross-entropy loss \mathcal{L}_{NLL} is used as the supervision criterion.

Teacher ResNet110: 93.91%			
Method	1-bit	2-bit	4-bit
Pre-trained FP student ResNet20: 92.21%			
Label-free FAQD	89.97%	91.40%	92.55%
FAQD with Supervision	90.92%	91.93%	92.74%
Pre-trained FP student ResNet56: 93.31%			
Label-free FAQD	92.34%	92.91%	93.52%
FAQD with Supervision	92.38%	93.14%	93.77%

TABLE III: Fine-tuning knowledge distillation for quantization of all convolutional layers.

For end-to-end quantization, we found that MSE loss performs better than KL loss. Adam optimization struggles to reach acceptable performance on end-to-end quantization (with either KL or MSE loss). We further test the performance of FAQD on larger dataset CIFAR-100 where an FP ResNet 164 teaches a quantized ResNet110. We report the accuracies for both label-free and label-present supervision. We evaluate FAQD on both fine-tuning quantization and end-to-end quantization.

In the ResNet experiment, the teacher ResNet164 has 74.50% testing accuracy. For the pretrained FAQD, the FP student ResNet110 has 72.96% accuracy. As shown in table VI

Teacher ResNet110: 93.91%			
Method	1-bit	2-bit	4-bit
FP student ResNet20: 92.21 %			
Label-free FAQD	89.88%	91.23%	92.19%
FAQD with Supervision	90.56%	91.65%	92.43%
FP student ResNet56: 93.31 %			
Label-free FAQD	91.36%	92.41%	92.72%
FAQD with Supervision	91.62%	92.44%	92.88%

TABLE IV: End-to-end FAQD. The accuracy of 4-bit label-free quantization nears or surpasses FP ResNet20/56.

Teacher ResNet164: 74.50%			
Initial FP student ResNet110: 72.96%			
Method	1-bit	2-bit	4-bit
label-free FAQD	73.33%	75.02%	75.78%
FAQD with Supervision	73.35%	75.24%	76.10%

TABLE V: Fine-tuning quantization of ResNet-110 on CIFAR-100. The 4-bit label-free quantized student surpasses the teacher.

Teacher ResNet164: 74.50%			
Method	1-bit	2-bit	4-bit
label-free FAQD	72.78%	74.35%	74.90%
FAQD with Supervision	73.35%	74.40%	75.31%

TABLE VI: End-to-end FAQD of ResNet110 on CIFAR-100. The accuracy of 4-bit label-free quantization surpasses 72.96% of FP ResNet110 and is close to FP ResNet164.

and table V, FAQD has surprisingly superior performance on CIFAR-100. The binarized student almost reaches the accuracy of FP model, and the 4-bit model surpasses the FP teacher.

B. Full Quantization

In this section, we extend our results to full quantization where the activation function is also quantized. As shown in table VII, the 4W4A fine-tuning quantization has accuracy similar to float ResNet20. Meanwhile, we fill in the long existing performance gap [9] when reducing precision from 1W2A to 1W1A on CIFAR-10 dataset, as the accuracy drop is linear (with respect to activation precision) and small.

CIFAR-10 (FP ResNet20: 92.21%)					
Model	pre-trained	1W1A	1W2A	1W4A	4W4A
ResNet20	No	87.51%	88.01%	90.71%	91.77%
ResNet20	Yes	88.16%	88.62%	91.52%	92.21%
CIFAR-100 (FP ResNet110: 72.96 %)					
Model	pre-trained	1W4A	4W4A		
ResNet110	No	68.82%	71.85%		
ResNet110	Yes	70.03%	72.09%		

TABLE VII: Full quantization on CIFAR-10 and CIFAR-100 for both end-to-end quantization and fine-tuning.

IV. FAST FEATURE AFFINITY LOSS

A. Proposed Method

Despite the significant increase of KD performance, we note that introducing FA loss will increase the training time. If we normalize the feature maps by row beforehand, computing

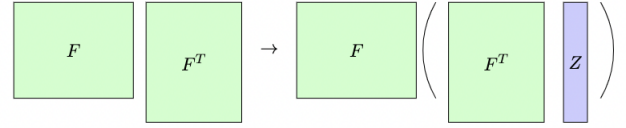


Fig. 3: Fast feature affinity loss with a low-rank random matrix Z .

FA loss between multiple intermediate feature maps can be expensive.

$$\mathcal{L}_{fa}(F_1, F_2) = \|F_1 F_1^T - F_2 F_2^T\|_2^2. \quad (12)$$

As we freeze the pre-trained teacher, feature map of the teacher model $F_1 = f^T(\mathbf{x})$ is a constant, in contrast to student feature map $F_1 = f^S(\Theta, \mathbf{x})$. Denote $\mathbf{S}_1 = F_1 F_1^T \in \mathbb{R}^{WH \times WH}$ and $g(\Theta, \mathbf{x}) = f^S(\Theta, \mathbf{x}) [f^S(\Theta, \mathbf{x})]^T$. The feature affinity can be formulated as

$$\mathcal{L}_{fa}(\Theta) = \frac{1}{|\mathcal{X}|} \sum_{\mathbf{x} \in \mathcal{X}} \|\mathbf{S}_1 - g(\Theta, \mathbf{x})\|_2^2. \quad (13)$$

Computing \mathbf{S}_1 and $g(\Theta, X)$ requires $\mathcal{O}(W^2 H^2 C)$ complexity each (C is the number of channels), which is quite expensive. We introduce a random estimator of $\mathcal{L}_{ffa}(\Theta)$:

$$\mathcal{L}_{fa}(F_1, F_2, \mathbf{z}) = \frac{1}{|\mathcal{X}|} \sum_{\mathbf{x} \in \mathcal{X}} \|(\mathbf{S}_1 - g(\Theta, \mathbf{x}))\mathbf{z}\|_2^2, \quad (14)$$

where $\mathbf{z} \in \mathbb{R}^{HW}$ is a vector with i.i.d unit normal components $N(0, 1)$. We show below that Eq. (14) is an unbiased estimator of FA loss (13).

Proposition 1:

$$\mathbb{E}_{\mathbf{z} \sim N(0,1)}[\mathcal{L}_{fa}(F_1, F_2, \mathbf{z})] = \mathcal{L}_{fa}(\Theta).$$

This estimator can achieve computing complexity $\mathcal{O}(HWC)$ by performing two matrix-vector multiplication $F_1 (F_1^T \mathbf{z})$. We define the Fast Feature Affinity (FFA) loss to be the k ensemble of (14):

$$\mathcal{L}_{ffa,k}(\Theta) = \frac{1}{|\mathcal{X}|} \sum_{\mathbf{x} \in \mathcal{X}} \frac{1}{k} \|(\mathbf{S}_1 - g(\Theta, \mathbf{x}))Z_k\|_2^2 \quad (15)$$

where $Z_k \in \mathbb{R}^{HW \times k}$ with i.i.d $\mathcal{N}(0, 1)$ components, and we have $k \ll WH$. The computational complexity of $\mathcal{L}_{ffa,k}(\Theta)$ is $\mathcal{O}(kWHC)$.

Finally, we remark that FFA loss can accelerate computation of pairwise Euclidean distance in dimensional reduction such as in (7). The popular way to compute the pairwise distance of rows for a matrix $A \in \mathbb{R}^{n \times c}$ is to broadcast the vector of row norms and compute AA^T . Given the row norm vector $v = (\|A_1\|^2, \dots, \|A_n\|^2)$, the similarity matrix (\mathbf{S}_{ij}) , $\mathbf{S}_{ij} = \|A_i - A_j\|^2$, is computed as

$$\mathbf{S} = \mathbf{1} \otimes v - 2AA^T + v \otimes \mathbf{1}.$$

The term $2AA^T$ can be efficiently approximated by FFA loss.

B. Experimental Results

We test Fast FA loss on CIFAR-15. As mentioned in the previous section, ResNet-20 has 3 residual blocks. The corresponding width and height for feature maps are 32, 16, and 8, $H = W$ for all groups, so the dimension (HW) of similarity matrices are 1024, 256, and 64. We test the fast FA loss with dimensions 1, 6, and 10. The results are shown in table VIII. Meanwhile, the FFA has much training time for each step. When $k = 1$, the accuracies are inconsistent due to large variance. With too few samples in the estimator, the fast FA norm is too noisy and jeopardize the distillation. When $k = 6$, the fast FA loss stabilizes and shows a significant improvement from the baseline, $\mathcal{L} = \mathcal{L}_{MSE} + \mathcal{L}_{CE}$ as in table II. When k increases to 10, the performance fast FA loss is comparable with the exact FA loss (table IV). Moreover, we experiment with the time consumption for computing FA loss and FFA loss. We plot the time in log scale vs. H , ($H = W$) for feature maps. The theoretical time complexity for computing exact FA loss is $\mathcal{O}(H^4)$ and that for computing FFA loss is $\mathcal{O}(H^2)$. We see that figure 4(a) agrees with the theoretical estimate. The larger the H , the more advantage

Model	k	2W32A	4W32A	4W4A
Fast FA Loss Accuracy				
ResNet20	1	90.83±2.75%	91.83±3.01%	90.32± 2.35%
ResNet20	5	91.37%	92.14%	91.12%
ResNet20	15	91.45%	92.39%	91.53%
Fast FA Loss Computing Time Per Step				
ResNet20	1	44 ms	65 ms	187 ms
ResNet20	5	46 ms	66 ms	188 ms
ResNet20	15	48 ms	68 ms	190 ms
Exact FA Loss Computing Time Per Step				
ResNet20	N/A	60 ms	80 ms	205 ms

TABLE VIII: Test FFA loss for different k on CIFAR-10 (end-to-end quantization). As k increases, the performance is approaching the exact FA loss. The 4-bit projection is more time consuming than 2-bit. STE and α update in full-quantization add extra time in milliseconds (ms).

the FFA loss. For (medical) images with resolutions in the thousands, the FFA loss will have significant computational savings.

C. Theoretical Analysis of FFA Loss

As shown in proposition 4.1, the FFA loss is a k ensemble unbiased estimator of FA loss. By the strong law of large numbers, the FFA loss converges to the exact FA loss with probability 1.

Theorem 4.1: For given Θ , suppose that $|\mathcal{L}_{fa}(\Theta)| \leq \infty$, then

$$\forall \epsilon > 0, \exists N \text{ s.t. } \forall k > N, |\mathcal{L}_{ffa,k}(\Theta) - \mathcal{L}_{fa}(\Theta)| < \epsilon.$$

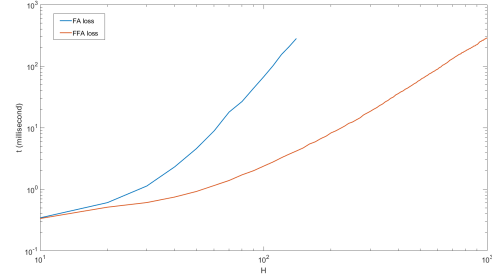
Namely, the FFA loss converges to FA loss pointwise:

$$\forall \Theta, \lim_{k \rightarrow \infty} \mathcal{L}_{ffa,k}(\Theta) = \mathcal{L}_{fa}(\Theta).$$

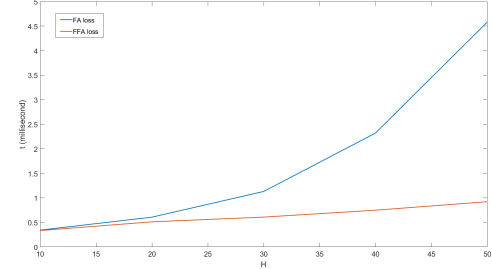
We also establish the following error bound for finite k .

Proposition 2:

$$\mathbb{P}(|\mathcal{L}_{ffa,k}(\Theta) - \mathcal{L}_{fa}(\Theta)| > \epsilon) \leq \frac{C}{\epsilon^2 k},$$



(a) Log-log plot for inference time of FA loss and FFA loss.



(b) Zoomed in plot for inference time of FA loss and FFA loss.

Fig. 4: Plots for inference time of FA loss and FFA loss with $k = 1$.

where $C \leq 3 \|\mathcal{L}_{fa}(\Theta)\|_2^4$.

Proposition 4.2 says that the probability that the FFA estimation has an error beyond a target value decays like $\mathcal{O}(\frac{1}{k})$. The analysis guarantees the accuracy of FFA loss as an efficient estimator of FA loss. Another question one might ask is whether minimizing the FFA loss is equivalent to minimizing the FA loss. Denote $\Theta^* = \arg \min L_{fa}(\Theta)$ and $\Theta_k^* = \arg \min L_{ffa,k}(\Theta)$, and assume the minimum is unique for each function. In order to substitute FA loss by FFA loss, one would hope that Θ_k^* converges to Θ^* . Unfortunately, the point-wise convergence in Theorem 4.1 is not sufficient to guarantee the convergence of the optimal points, as a counter-example can be easily constructed. In the rest of this section, we show that such convergence can be established under an additional assumption.

Theorem 4.2 (Convergence in the general case): Suppose that $\mathcal{L}_{ffa,k}(\Theta)$ converges to $\mathcal{L}_{fa}(\Theta)$ uniformly, that is

$$\forall \epsilon > 0, \exists N \text{ s.t. } \forall k > N, |\mathcal{L}_{ffa,k}(\Theta) - \mathcal{L}_{fa}(\Theta)| < \epsilon$$

$\forall \Theta$ and

$$|\mathcal{L}_{fa}(\Theta)| \leq \infty, \forall \Theta.$$

Then

$$\lim_{k \rightarrow \infty} \|\Theta_k^* - \Theta^*\|^2 = 0. \quad (16)$$

The uniform convergence can be relaxed if \mathcal{L}_{fa} is convex in Θ . We would like to present a consequence of Theorem 4.2.

Corollary 4.2.1 (Convergence in the convex case): Suppose that $L_{fa} : \mathbb{R}^n \rightarrow \mathbb{R}$ is convex and L -smooth, and that there $\exists M$ such that $\|\Theta_k^*\| \leq M, \forall k$. Then, $\forall k$, $\mathcal{L}_{ffa,k}$ is also convex, and $\lim_{k \rightarrow \infty} \|\Theta_k^* - \Theta^*\|^2 = 0$.

V. CONCLUSION

We presented FAQD, a feature assisted (FA) knowledge distillation method for training-aware quantization. It couples MSE loss with FA loss and significantly improves the accuracy of the quantized student. FAQD works for both weight only and full quantization, and outperforms baseline Resnets on CIFAR-10 and CIFAR-100. We also analyzed an efficient randomized approximation (FFA) to the FA loss for feature maps with large dimensions. This theoretically founded FFA loss benefits training models on high resolution images.

VI. APPENDIX

Proof of Theorem 2.1: It suffices to prove that for any set of n unit vectors in \mathbb{R}^d , there is a linear map nearly preserving pairwise angular distances, because the angular distance is scale-invariant.

Let T be a linear transformation induced by a random Gaussian matrix $\frac{1}{\sqrt{k}}A \in \mathbb{R}^{k \times d}$ such that $T(\mathbf{F}) = \mathbf{F}A^T$. Define the events $\mathcal{A}_{ij}^- = \{T : (1-\epsilon)\|\mathbf{F}_i - \mathbf{F}_j\|^2 \leq \|T(\mathbf{F})_i - T(\mathbf{F})_j\|^2 \leq (1+\epsilon)\|\mathbf{F}_i - \mathbf{F}_j\|^2 \text{ fails}\}$ and $\mathcal{A}_{ij}^+ = \{T : (1-\epsilon)\|\mathbf{F}_i + \mathbf{F}_j\|^2 \leq \|T(\mathbf{F})_i + T(\mathbf{F})_j\|^2 \leq (1+\epsilon)\|\mathbf{F}_i + \mathbf{F}_j\|^2 \text{ fails}\}$.

Following the proof of the classical JL lemma in the Euclidean case [23], we have:

$$P(\mathcal{A}_{ij}^-) \leq 2e^{-\frac{(\epsilon^2 - \epsilon^3)k}{4}}, \quad P(\mathcal{A}_{ij}^+) \leq 2e^{-\frac{(\epsilon^2 - \epsilon^3)k}{4}}. \quad (17)$$

Let $\mathcal{B}_{ij} = \{T : |\mathbf{F}_i \cdot \mathbf{F}_j - T(\mathbf{F})_i \cdot T(\mathbf{F})_j| > \epsilon\}$, where \cdot is the shorthand for inner product. We show that $\mathcal{B}_{ij} \subset \mathcal{A}_{ij}^- \cup \mathcal{A}_{ij}^+$ for $\|\mathbf{F}_i\| = \|\mathbf{F}_j\| = 1$ by showing $\mathcal{A}_{ij}^{-C} \cap \mathcal{A}_{ij}^{+C} \subset \mathcal{B}_{ij}^C$.

If $\mathcal{A}_{ij}^{-C} \cap \mathcal{A}_{ij}^{+C}$ holds, we have

$$\begin{aligned} & 4T(\mathbf{F})_i \cdot T(\mathbf{F})_j \\ &= \|T(\mathbf{F})_i + T(\mathbf{F})_j\|^2 - \|T(\mathbf{F})_i - T(\mathbf{F})_j\|^2 \\ &\leq (1+\epsilon)\|\mathbf{F}_i + \mathbf{F}_j\|^2 - (1-\epsilon)\|\mathbf{F}_i - \mathbf{F}_j\|^2 \\ &= 4\mathbf{F}_i \cdot \mathbf{F}_j + 2\epsilon(\|\mathbf{F}_i\|_2^2 + \|\mathbf{F}_j\|^2) \\ &= 4\mathbf{F}_i \cdot \mathbf{F}_j + 4\epsilon. \end{aligned}$$

Therefore, $\mathbf{F}_i \cdot \mathbf{F}_j - T(\mathbf{F})_i \cdot T(\mathbf{F})_j \geq -\epsilon$. By a similar argument, we have $\mathbf{F}_i \cdot \mathbf{F}_j - T(\mathbf{F})_i \cdot T(\mathbf{F})_j \leq \epsilon$. Then we have $\mathcal{A}_{ij}^{-C} \cap \mathcal{A}_{ij}^{+C} \subset \mathcal{B}_{ij}^C$, and thus

$$\mathbb{P}(\mathcal{B}_{ij}) \leq \mathbb{P}(\mathcal{A}_{ij}^- \cup \mathcal{A}_{ij}^+) \leq 4 \exp\left\{-\frac{(\epsilon^2 - \epsilon^3)k}{4}\right\}$$

and

$$\mathbb{P}(\cup_{i < j} \mathcal{B}_{ij}) \leq \sum_{i < j} \mathbb{P}(\mathcal{B}_{ij}) \leq 4n^2 \exp\left\{-\frac{(\epsilon^2 - \epsilon^3)k}{4}\right\}.$$

This probability is less than 1 if we take $k > \frac{16 \ln n}{\epsilon^2}$. Therefore, there must exist a T such that $\cap_{i < j} \mathcal{B}_{ij}^C$ holds, which completes the proof.

Proof of Proposition 4.1: Letting $N = WH$, $a_{ij} = (F_1 F_1^T)_{ij}$, and $b_{ij} = (F_2 F_2^T)_{ij}$ in equation (14), we have:

$$\begin{aligned} \mathbb{E}_z \mathcal{L}_{ffa}(F_1, F_2; 2) &= \mathbb{E}_z \sum_{i=1}^N \sum_{j=1}^N |a_{ij} - b_{ij}| z_j^2 \\ &= \mathbb{E}_z \sum_{i=1}^N \sum_{j=1}^N |a_{ij} - b_{ij}|^2 z_j^2 + 2 \sum_{j \neq k} |a_{ij} - b_{ij}| |a_{ik} - b_{ik}| z_j z_k \\ &= \mathbb{E}_z \sum_{i=1}^N \sum_{j=1}^N |a_{ij} - b_{ij}|^2 z_j^2 + 2 \sum_{i=1}^N \sum_{j \neq k} |a_{ij} - b_{ij}| |a_{ik} - b_{ik}| z_j z_k \\ &= \sum_{i=1}^N \sum_{j=1}^N |a_{ij} - b_{ij}|^2 \mathbb{E}_z z_j^2 \\ &\quad + 2 \sum_{i=1}^N \sum_{j \neq k} |a_{ij} - b_{ij}| |a_{ik} - b_{ik}| \mathbb{E}_z z_j z_k \\ &= \sum_{i=1}^N \sum_{j=1}^N |a_{ij} - b_{ij}|^2 = \mathcal{L}_{fa}(F_1, F_2; 2). \end{aligned}$$

Proof of Theorem 4.1: Given a Gaussian matrix $Z_k = [\mathbf{z}_1, \dots, \mathbf{z}_k] \in \mathbb{R}^{n \times k}$,

$$\mathcal{L}_{ffa,k}(\Theta) = \frac{1}{k} \sum_{l=1}^k \mathcal{L}_{ffa}(F_1, F_2, \mathbf{z}_l).$$

For any fixed Θ , $\mathcal{L}_{ffa}(F_1, F_2, \mathbf{z}_l)$, $l = 1, \dots, k$, are i.i.d random variables. Suppose the first moment of each random variable is finite, by the strong law of large numbers, $\mathcal{L}_{ffa,k}(\Theta)$ converges to $\mathbb{E}[\mathcal{L}_{ffa}(F_1, F_2, \mathbf{z}_1)]$ almost surely. In other words, $\lim_{k \rightarrow \infty} \mathcal{L}_{ffa,k}(\Theta) = \mathcal{L}_{fa}(\Theta)$ with probability 1.

Proof of Proposition 4.2: By Chebyshev's inequality, we have

$$\mathbb{P}(|\mathcal{L}_{ffa,k}(\Theta) - \mathbb{E}[\mathcal{L}_{ffa,k}(\Theta)]| > \epsilon) \leq \frac{\text{Var}(\mathcal{L}_{ffa,k}(\Theta))}{\epsilon^2} = \frac{\text{Var}(\mathcal{L}_{ffa}(F_1, F_2, \mathbf{z}_1))}{\epsilon^2 k}. \quad (18)$$

In order to estimate

$$\text{Var}(\mathcal{L}_{ffa}(F_1, F_2, \mathbf{z}_1)) = \mathbb{E}[\mathcal{L}_{ffa}^2(F_1, F_2, \mathbf{z}_1)] - (\mathbb{E}[\mathcal{L}_{ffa}(F_1, F_2, \mathbf{z}_1)])^2, \quad (19)$$

it suffices to estimate

$$\begin{aligned} & \mathbb{E}[\mathcal{L}_{ffa}^2(F_1, F_2, \mathbf{z}_1)] = \\ & \mathbb{E}_z \left(\sum_{i=1}^N \sum_{j=1}^N |a_{ij} - b_{ij}|^2 z_j^2 + \sum_{i=1}^N \sum_{j \neq k} |a_{ij} - b_{ij}| |a_{ik} - b_{ik}| z_j z_k \right)^2 \end{aligned}$$

which equals (as cross terms are zero):

$$\begin{aligned} &= \mathbb{E}_z \left(\sum_{i=1}^N \sum_{j=1}^N |a_{ij} - b_{ij}|^2 z_j^2 \right)^2 \\ &\quad + \left(\sum_{i=1}^N \sum_{j \neq k} |a_{ij} - b_{ij}| |a_{ik} - b_{ik}| z_j z_k \right)^2. \end{aligned}$$

Direct computation yields:

$$\begin{aligned} & \sum_{i=1}^N \sum_{j=1}^N |a_{ij} - b_{ij}|^4 z_j^4 + \sum_{i=1}^N \sum_{j=1}^N \sum_{l \neq i}^N |a_{ij} - b_{ij}|^2 |a_{lj} - b_{lj}|^2 z_j^4 \\ & + 2 \sum_{i=1}^N \sum_{j=1}^N \sum_{l \neq j}^N |a_{ij} - b_{ij}|^2 |a_{il} - b_{il}|^2 z_j^2 z_l^2 \\ & + \sum_{i=1}^N \sum_{j=1}^N \sum_{k=1}^N \sum_{l \neq j}^N |a_{ij} - b_{ij}|^2 |a_{kl} - b_{kl}|^2 z_j^2 z_l^2 \end{aligned}$$

Notice that $\mathbb{E}[z_i^4] = 3$. Taking $\mathbb{E}[\cdot]$, we derive the upper bound $3\|\mathcal{L}_{fa}\|_2^4$.

Proof of Theorem 4.2: Since $\lim_{k \rightarrow \infty} \mathcal{L}_{ffa,k}(\Theta^*) = \mathcal{L}_{fa}(\Theta^*)$, it suffices to show that

$$\lim_{k \rightarrow \infty} \inf_{\Theta} \mathcal{L}_{ffa,k}(\Theta) = \mathcal{L}_{fa}(\Theta^*).$$

Note that

$$\forall \Theta, \lim_{k \rightarrow \infty} \mathcal{L}_{ffa,k}(\Theta) = \mathcal{L}_{fa}(\Theta) \leq \mathcal{L}_{fa}(\Theta^*).$$

Then,

$$\mathcal{L}_{fa}(\Theta^*) \geq \lim_{k \rightarrow \infty} \inf_{\Theta} \mathcal{L}_{ffa,k}(\Theta).$$

On the other hand, for arbitrary $\epsilon > 0$, we have:

$$\exists N \text{ s.t. } \forall k > N \quad |\mathcal{L}_{ffa,k}(\Theta) - \mathcal{L}_{fa}(\Theta)| < \frac{\epsilon}{2}, \forall \Theta$$

and there exists a sequence $\{\Theta_k\}$ s.t.

$$\mathcal{L}_{ffa,k}(\Theta_k) < \inf_{\Theta} \mathcal{L}_{ffa,k}(\Theta) + \frac{\epsilon}{2}.$$

Note that $|\mathcal{L}_{ffa,k}(\Theta_k) - \mathcal{L}_{fa}(\Theta_k)| < \frac{\epsilon}{2}$ for $k > N$, so:

$$\mathcal{L}_{fa}(\Theta^*) - \epsilon \leq \mathcal{L}_{fa}(\Theta_k) - \epsilon < \inf_{\Theta} \mathcal{L}_{ffa,k}(\Theta), \quad \forall k > N.$$

Since ϵ is arbitrary, taking $k \rightarrow \infty$, we have

$$\mathcal{L}_{fa}(\Theta^*) \leq \lim_{k \rightarrow \infty} \inf_{\Theta} \mathcal{L}_{ffa,k}(\Theta).$$

Proof of Corollary 4.2.1: For readability, we shorthand:

$\mathcal{L}_{ffa,k} = f_k$ and $\mathcal{L}_{fa} = f$. Let

$$\mathbf{H} = \frac{\nabla^2 f}{\nabla \Theta \nabla \Theta^T} \succcurlyeq \mathbf{0} \in \mathcal{R}^{n \times n}$$

be the Hessian matrix of FA loss, which is positive semi-definite by convexity of L_{fa} . Then,

$$\frac{\nabla^2 f_k}{\nabla \Theta \nabla \Theta^T} = Z_k^T \mathbf{H} Z_k \succcurlyeq \mathbf{0} \in \mathbb{R}^{k \times k}$$

which implies the convexity of f_k for all k . Moreover, it is clear that f_k is smooth for all k since

$$\begin{aligned} \|\nabla f_k(\mathbf{x}) - \nabla f_k(\mathbf{y})\| &= \|Z_k(\nabla f(\mathbf{x}) - \nabla f(\mathbf{y}))\| \\ &\leq L \cdot \|Z_k\| \cdot \|\mathbf{x} - \mathbf{y}\|. \end{aligned} \quad (20)$$

We note that f_k is also smooth. Although we cannot claim equi-smoothness since we cannot bound $\|Z_k\|$ uniformly in k , the above is sufficient for us to prove the desired result.

For $\forall k$, given any initial parameters Θ^0 , by smoothness and convexity of f_k , it is well-known that

$$\|\Theta_k^t - \Theta_k^*\| \leq \|\Theta^0 - \Theta_k^*\|$$

where Θ_k^t is the parameter we arrive after t steps of gradient descent. Hence, we can pick a compact set $\mathbf{K} = \overline{B_R(\Theta^*)}$ for R large enough such that $\{\Theta_k\}_{k=1}^\infty \subset \mathbf{K}$ (denote $\Theta_\infty^* = \Theta^*$). Now, it suffices to prove f_k converges to f uniformly on K . In fact, f_k converges to f on any compact set. To begin with, we state a known result from functional analysis ([5], [12]):

Lemma 6.1: (Uniform boundness and equi-Lipschitz) Let \mathcal{F} be a family of convex function on \mathbb{R}^n and $K \subset \mathbb{R}^n$ be a compact subset. Then, \mathcal{F} is equi-bounded and equi-Lipschitz on K .

This result is established in any Banach space in [12], so it automatically holds in finite dimensional Euclidean space. By Lemma 6.1, we have that the sequence $\{f_k\}_{k=1}^\infty$, where $f_\infty = f$, is equi-Lipschitz. $\forall \epsilon > 0, \exists \delta > 0$ s.t. $|f_k(x) - f_k(y)| < \epsilon$ for all k and $x, y \in K$ when $|x - y| < \delta$. Since $\{B(x, \delta)\}_{x \in K}$ forms an open cover for K , we have a finite sub-cover $\{B(x_j, \delta)\}_{j=1}^m$ of K . Since there are finitely many points x_j , there exists N_ϵ such that

$$\forall k > N_\epsilon, \quad |f_k(x_j) - f(x_j)| < \epsilon, \text{ for } j = 1, \dots, m.$$

For any $x \in K, x \in B(x_{j^*}, \delta)$ for some j^* . For all $k > N_\epsilon$, we have

$$\begin{aligned} |f_k(x) - f(x)| &\leq \\ |f_k(x) - f_k(x_{j^*})| &+ |f_k(x_{j^*}) - f(x_{j^*})| + |f(x_{j^*}) - f(x)| \\ &\leq (2\tilde{L} + 1)\epsilon \end{aligned} \quad (21)$$

where \tilde{L} is the Lipschitz constant for equi-Lipschitz family. Therefore, f_k converges to f uniformly on K .

REFERENCES

- [1] Luca Becchetti, Marc Bury, Vincent Cohen-Addad, Fabrizio Grandoni, and Chris Schwiegelshohn. Oblivious dimension reduction for k-means: beyond subspaces and the Johnson-Lindenstrauss lemma. In *Proceedings of the 51st annual ACM SIGACT symposium on theory of computing*, pages 1039–1050, 2019.
- [2] Yoshua Bengio, Nicholas Léonard, and Aaron Courville. Estimating or propagating gradients through stochastic neurons for conditional computation. *arXiv preprint arXiv:1308.3432*, 2013.
- [3] Zhaowei Cai, Xiaodong He, Jian Sun, and Nuno Vasconcelos. Deep learning with low precision by half-wave gaussian quantization. In *Proceedings of the IEEE conference on computer vision and pattern recognition*, pages 5918–5926, 2017.
- [4] Jungwook Choi, Zhuo Wang, Swagath Venkataramani, Pierce I-Jen Chuang, Vijayalakshmi Srinivasan, and Kailash Gopalakrishnan. Pact: Parameterized clipping activation for quantized neural networks. *arXiv preprint arXiv:1805.06085*, 2018.
- [5] S Cobzas. Lipschitz properties of convex mappings. *Adv. Oper. Theory*, 2(1):21–49, 2017.
- [6] Matthieu Courbariaux, Yoshua Bengio, and Jean-Pierre David. Binaryconnect: Training deep neural networks with binary weights during propagations. *Advances in neural information processing systems*, 28, 2015.
- [7] Tim Dockhorn, Yaoliang Yu, Eyyüb Sari, Mahdi Zolnouri, and Vahid Partovi Nia. Demystifying and generalizing binaryconnect. *Advances in Neural Information Processing Systems*, 34:13202–13216, 2021.
- [8] Ruihao Gong, Xianglong Liu, Shenghu Jiang, Tianxiang Li, Peng Hu, Jiazhen Lin, Fengwei Yu, and Junjie Yan. Differentiable soft quantization: Bridging full-precision and low-bit neural networks. In *Proceedings of the IEEE/CVF International Conference on Computer Vision*, pages 4852–4861, 2019.
- [9] Ruihao Gong, Xianglong Liu, Shenghu Jiang, Tianxiang Li, Peng Hu, Jiazhen Lin, Fengwei Yu, and Junjie Yan. Differentiable soft quantization: Bridging full-precision and low-bit neural networks. In *Proceedings of the IEEE/CVF International Conference on Computer Vision*, pages 4852–4861, 2019.
- [10] Geoffrey Hinton, Oriol Vinyals, Jeff Dean, et al. Distilling the knowledge in a neural network. *arXiv preprint arXiv:1503.02531*, 2(7), 2015.
- [11] William B Johnson, Joram Lindenstrauss, and Gideon Schechtman. Extensions of Lipschitz maps into Banach spaces. *Israel Journal of Mathematics*, 54(2):129–138, 1986.
- [12] Mohamed Jouak and Lionel Thibault. Equicontinuity of families of convex and concave-convex operators. *Canadian Journal of Mathematics*, 36(5):883–898, 1984.
- [13] Jangho Kim, Yash Bhalgat, Jinwon Lee, Chirag Patel, and Nojun Kwak. Qkd: Quantization-aware knowledge distillation. *arXiv preprint arXiv:1911.12491*, 2019.
- [14] Taehyeon Kim, Jaehoon Oh, NakYil Kim, Sangwook Cho, and Se-Young Yun. Comparing kullback-leibler divergence and mean squared error loss in knowledge distillation. pages 2628–2635, 2021.
- [15] Yuhang Li, Ruihao Gong, Xu Tan, Yang Yang, Peng Hu, Qi Zhang, Fengwei Yu, Wei Wang, and Shi Gu. Brecq: Pushing the limit of post-training quantization by block reconstruction. *arXiv preprint arXiv:2102.05426*, 2021.
- [16] Zhijian Li, Bao Wang, and Jack Xin. An integrated approach to produce robust deep neural network models with high efficiency. In *International Conference on Machine Learning, Optimization, and Data Science*, pages 451–465. Springer, 2021.
- [17] Ziang Long, Penghang Yin, and Jack Xin. Recurrence of optimum for training weight and activation quantized networks. *Applied and Computational Harmonic Analysis*, 62:41–65, 2023.
- [18] Konstantin Makarychev, Yury Makarychev, and Ilya Razenshteyn. Performance of Johnson-Lindenstrauss transform for k-means and k-medians clustering. In *Proceedings of the 51st Annual ACM SIGACT Symposium on Theory of Computing*, pages 1027–1038, 2019.
- [19] Antonio Polino, Razvan Pascanu, and Dan Alistarh. Model compression via distillation and quantization. *arXiv preprint arXiv:1802.05668*, 2018.
- [20] Dinesh Ramasamy and Upamanyu Madhoo. Compressive spectral embedding: sidestepping the svd. *Advances in neural information processing systems*, 28, 2015.
- [21] Mohammad Rastegari, Vicente Ordonez, Joseph Redmon, and Ali Farhadi. Xnor-net: Imagenet classification using binary convolutional neural networks. In *European conference on computer vision*, pages 525–542. Springer, 2016.
- [22] Nicolas Tremblay, Gilles Puy, Rémi Gribonval, and Pierre Vandergheynst. Compressive spectral clustering. In *International conference on machine learning*, pages 1002–1011. PMLR, 2016.
- [23] Santosh S Vempala. *The random projection method*, volume 65. American Mathematical Soc., 2005.
- [24] Li Wang, Dong Li, Yousong Zhu, Lu Tian, and Yi Shan. Dual super-resolution learning for semantic segmentation. In *Proceedings of the IEEE/CVF Conference on Computer Vision and Pattern Recognition*, pages 3774–3783, 2020.
- [25] Biao Yang, Fanghui Xue, Yinyong Qi, and Jack Xin. Improving efficient semantic segmentation networks by enhancing multi-scale feature representation via resolution path based knowledge distillation and pixel shuffle. In *Proceedings of the 16th International Symposium on Visual Computing*, pages 325–336. Springer, Cham, 2021.
- [26] Junho Yim, Donggyu Joo, Jihoon Bae, and Junmo Kim. A gift from knowledge distillation: Fast optimization, network minimization and transfer learning. In *Proceedings of the IEEE Conference on Computer Vision and Pattern Recognition*, pages 4133–4141, 2017.
- [27] Penghang Yin, Jiancheng Lyu, Shuai Zhang, Stanley Osher, Yingyong Qi, and Jack Xin. Understanding straight-through estimator in training activation quantized neural nets. in *Proceedings of International Conference on Learning Representations (ICLR)*, 2019.
- [28] Penghang Yin, Shuai Zhang, Jiancheng Lyu, Stanley Osher, Yingyong Qi, and Jack Xin. Binaryrelax: A relaxation approach for training deep neural networks with quantized weights. *SIAM Journal on Imaging Sciences*, 11(4):2205–2223, 2018.
- [29] Penghang Yin, Shuai Zhang, Jiancheng Lyu, Stanley Osher, Yingyong Qi, and Jack Xin. Blended coarse gradient descent for full quantization of deep neural networks. *Research in the Mathematical Sciences*, 6(1):1–23, 2019.
- [30] Sergey Zagoruyko and Nikos Komodakis. Paying more attention to attention: Improving the performance of convolutional neural networks via attention transfer. *arXiv preprint arXiv:1612.03928*, 2016.
- [31] Hongyang Zhang, Yaodong Yu, Jiantao Jiao, Eric Xing, Laurent El Ghaoui, and Michael Jordan. Theoretically principled trade-off between robustness and accuracy. In *International conference on machine learning*, pages 7472–7482. PMLR, 2019.